Published online 14 December 2012 *Nucleic Acids Research, 2013, Vol. 41, No. 3* ***1533–1543***
doi:10.1093/nar/gks1232

A *cis*-element with mixed G-quadruplex structure of NPGPx promoter is essential for nucleolin-mediated transactivation on non-targeting siRNA stress

Pei-Chi Wei[1,2], Zi-Fu Wang[3,4], Wen-Ting Lo[2,5], Mei-I Su[5], Jin-Yuh Shew[1,2,*], Ta-Chau Chang[3,4,*] and Wen-Hwa Lee[2,6,*]

[1]Graduate Institute of Life Sciences, National Defense Medical Center, 11490 Taipei, Taiwan, [2]Genomics Research Center, 11529 Taipei, [3]Institute of Atomic and Molecular Sciences, Academia Sinica, 11529 Taipei, [4]Department of Chemistry, National Taiwan University, 11529 Taipei, [5]Institute of Biological Chemistry, Academia Sinica, 11529 Taipei, Taiwan and [6]Department of Biological Chemistry, University of California, Irvine, California, USA

Received September 26, 2012; Revised and Accepted October 31, 2012

ABSTRACT

We reported that non-targeting siRNA (NT-siRNA) stress induces non-selenocysteine containing phospholipid hydroperoxide glutathione peroxidase (NPGPx) expression to cooperate with exoribonuclease XRN2 for releasing the stress [Wei,P.C., Lo,W.T., Su,M.I., Shew,J.Y. and Lee,W.H. (2011) Non-targeting siRNA induces NPGPx expression to cooperate with exoribonuclease XRN2 for releasing the stress. *Nucleic Acids Res*., 40, 323–332]. However, how NT-siRNA stress inducing NPGPx expression remains elusive. In this communication, we showed that the proximal promoter of NPGPx contained a mixed G-quadruplex (G4) structure, and disrupting the structure diminished NT-siRNA induced NPGPx promoter activity. We also demonstrated that nucleolin (NCL) specifically bonded to the G4-containing sequences to replace the originally bound Sp1 at the NPGPx promoter on NT-siRNA stress. Consistently, overexpression of NCL further increased NPGPx promoter activity, whereas depletion of NCL desensitized NPGPx promoter to NT-siRNA stress. These results suggest that the *cis*-element with mixed G4 structure at the NPGPx promoter plays an essential role for its transactivation mediated by NCL to release cells from NT-siRNA stress.

INTRODUCTION

G-quadruplex, also called G4, is a DNA secondary structure composed by four times of $G_{2–4}$ repeats with nucleotides flanking within one strand of DNA (1). The G4 structure is first described as a single-stranded DNA containing short G-rich motifs, which can self-associate at physiological salt concentration to make into four stranded fashion (2). G-rich DNA sequences like $[d(T_nG_4)]_4$, which contains four repeats with four serial guanines flanked by thymidine, can be stabilized in the presence of monovalent cations, Na^+ and K^+ (3). G4 has a variety of structures depending on either topology, length of flanking nucleotides or guanine repeating times (4). The G4 structure has been found in immunoglobulin switch region (5); virus genome (6); and promoters such as c-Myc (7), HIF-1 (8), VEGF (9), KRAS (10), BCL2 (11) and chromosome telomere (12).

G4 topology can be generally classified into (i) parallel; (ii) anti-parallel; and (iii) mixed parallel/antiparallel according to the parallel status of each G column (13). Besides, the length of the side loop between the second and third G column is varied (from 2 to 26 flanking nucleotides), which may feature G4 with different side-chain conformation and flexibility (14). For example, the G4 in c-Myc promoter is parallel with six flanking nucleotides, whereas the G4 in hTERT promoter contains a 26-nucleotide side chain (14). It has been demonstrated that the *cis*-element of G4 participates in gene regulation. For example, a G-rich 27-base-pair element, NHE III_1,

*To whom correspondence should be addressed. Tel: +949 824 4492; Fax: +886 227 898 777; Email: whlee@uci.edu
Correspondence may also be addressed to Jin-Yuh Shew. Tel: +886 2 2789 1255; Fax: +886 227 898 777; Email: jyshew@gate.sinica.edu.tw
Correspondence may also be addressed to Ta-Chau Chang. Tel: +886 2 2366 8231; Fax: +886 227 898 777; Email: tcchang@po.iams.sinica.edu.tw

The authors wish to be known that, in their opinion, the first two author should be regarded as joint First Author.

locating at −142 to −115 base pairs upstream of the c-Myc P1 promoter contributes 80–90% of c-Myc transcription activity (15–18). A single G to A mutation of G4 destabilizes the G4-forming structure and results in the induction of c-Myc expression (19). In contrast, treatment with TMPyP4, a cationic porphyrin of G4 binding agent, stabilizes the mix parallel/antiparallel G4 structure (20) and is able to suppress c-Myc transcriptional activity (19). Apparently, this *cis*-element modulates either transcription activation or repression of the c-Myc transcription depending on its specific G4 structure feature.

It is known that G4-containing promoters recruit diverse transcription factors to regulate downstream gene expression. Nucleolin (NCL) is one of the key regulators for genes with G4 in promoters (21). NCL binds to the G4 in c-Myc promoter (21) and represses c-Myc expression (7). In contrast, NCL also can be a transactivator to regulate VEGF expression (22). NCL-containing G4-binding complexes are critical for gene regulation. For example, treatment of PMA facilities NCL binding to c-Jun (23), whereas genotoxic stresses including ionizing radiation induce p53-NCL complex formation (24) and also RPA–NCL interaction (25). These observations provide a plausible direction that stresses may activate G4-containing promoters through NCL-mediated transcriptional regulation. Previously, we have shown a novel non-targeting siRNA (NT-siRNA) stress, which induces NPGPx expression (26). NPGPx promoter is GC rich and may form a G4 structure. Furthermore, whether the induction of NPGPx expression by NT-siRNA stress is governed by a similar regulation is of interest to explore.

In this communication, we showed that the NPGPx promoter contains a mixed G4 *cis*-element, which is critical for NPGPx gene regulation. We further showed that NCL directly transactivated NPGPx expression through the mixed G4-containing promoter on NT-siRNA stress. Taken together with the previous results (26), it provides a plausible explanation of how NPGPx responses to NT-siRNA and releases the stress through activating endoribonuclease XRN2.

MATERIALS AND METHODS

Lentivirus production and infection

ShRNA-carrying lentivirus production was performed as previous described (26). To deplete NCL, WI38 cells were infected with lentivirus containing shRNA against NCL and selected with 2 μg/ml puromycin for 6 days. shNCL clones were purchased from National RNAi Core Facility, Academia Sinica, Taiwan.

DNA construction

NPGPx promoter (−3658 to +23) was cloned in pGL3-basic vector (Promega) with *Mlu*I and *Xho*I restriction enzyme. pGL3b-NPGPx-(−2356 to +23) reporter was generated from pGL3b-NPGPx-(−3654 to +23) with *Mlu*I and *Eco*RI to remove the distal promoter (−3658 to −2357) followed by Klenow fill-in procedure. pGL3b-NPGPx-(−1024 to +23) was generated using *Pst*I and *Mlu*I to cut out distal promoters. The following NPGPx promoters [NPGPx-(−1546 to +14), (−1432 to +14), (−1333 to +14), (−1163 to +14), (−120 to +14) and (−60 to +14)] were amplified by polymerase chain reaction (PCR) using primer pairs containing either *Xho*I or *Hind*III restriction sites on 5′ ends. These promoter DNA fragments were cloned into pGL3-basic vectors followed by *Xho*I and *Hind*III digestion to generate NPGPx reporters with different length. Mutated NPGPx promoters (with G/C to A/T substitution, illustrated in Figure 3a) were synthesized containing 5′ *Xho*I and 3′ *Hind*III cutting sites, and then cloned into pGL3-basic following restriction enzyme digestion. The pEGFP-NCL construct was kindly provided by professor Joseph T. Tseng (Institute of Bioinformatics, National Cheng Kung University, Taiwan), and NCL expression construct pNuc-1, 2, 3, 4-RGG-C4 was from Professor Nancy Maizel (Department of Immunology, University of Washington).

Western blot analysis

Cells were lyzed using RIPA buffer (50 mM Tris–HCl pH = 7.4, 150 mM NaCl, 2 mM EDTA, 50 mM NaF, 1% Nonidet P-40, 0.5% sodium deoxycholate, 0.1% SDS and 1 mM PMSF and 1 mM DTT) to extract protein, and following western blot analysis by using specific primary antibodies to probe NPGPx (GeneTex, GTX70266), GRP78 (BD, 610978), Sp1 (Santa Cruz, sc-59), c-Jun (GeneTex, GTX101135), NCL (Genetex, GTX13541) and α-tubulin (GeneTex, GTX11302).

RNA extraction, reverse transcription and quantitative real time PCR

Total RNA was extracted using Trizol reagent (Invitrogen) followed by DNAse treatment (Invitrogen, 18068-015, 1 unit DNAse/μg RNA), and the first strand of cDNA was reverse transcribed followed the manufacture's instruction (ABI, 4368814). NPGPx and S26 (as internal control) expression level was determined using SYBR-Green based quantitative real time PCR systems. Primers for NPGPx are as follows: forward 5′-GCAGGAGCAGGACTTCTA CGACTTC-3′ and reverse 5′-ACCGGTGACTGCAATC TTGCTAAAC3′; primers for S26 are as follows: forward 5′-CCGTGCCTCCAAGATGACAAAG-3′ and reverse 5′-ACTCAGCTCCTTACATGGGCTT-3′).

Reporter assay

NPGPx reporters and firefly luciferase reporter (pRL-TK) were co-transfected into 293T or WI38 cells using Lipofetamine™ 2000 reagent (Invitrogen). Luciferase activities and firefly luciferase activities were measured 48 h after transfection using Dual-Luciferase Reporter System (Promega).

Electrophoresis mobility shift assay

To generate biotynylated electrophoresis mobility shift assay (EMSA) probes, NPGPx promoter probe (−60 to +14) was amplified by PCR using pGL3b-NPGPx-(−3658 to +23) as template, and then ligate the dUTP-biotin at 3′ end mediated by TdT ligation (PIERCE, 89818).

Nuclear extract from shLuc-transduced WI38 cells (27) was mixed with either biotinylated, unlabled probe (cold-probe) or bacteria vector fragments (pBSK) at 37°C for 30 min in the presence of K^+ (50 mM). The DNA-nuclear protein complex was then separated in to 6% acrylamide (29:1) TBE gel and transferred to N-bond nylon membrane (PIERCE, 77016). Biotinyated probes were visualized using LightShift Chemiluminescent EMSA kit (PIERCE, 20148).

Chromatin immunoprecipitation

To assay the binding of transcription factors on NPGPx promoter, chromatin immunoprecipitation (ChIP) assay was performed following the protocol as previously described (28). In brief, 80% confluent cells were cross-linked by paraformaldehyde, lyzed in ChIP buffer (50 mM Tris-HCl pH = 7.9, 150 mM NaCl, 5 mM EDTA, 0.1% sodium-deoxycholate, 1% Triton-X-100, 0.5% Nonidet P-40, 1 mM PMSF and protease inhibitor), and immunoprecipitated the transcription factors using specific primary antibodies against NCL (GeneTex, GTX13541 or GTX30908), Sp1 (Santa Cruz, sc-59) or rabbit pre-immunized IgG (1 μg/1 mg lysate). The protein–DNA complex was reverse cross-linked, treated with proteinase K, and the DNA was eluted through chloroform/isopropanol filtration. PCR analysis was then applied to measure the amount of immunoprecipitated NPGPx proximal promoter (−60 to +14 of NPGPx promoter) using primers against the NPGPx proximal promoter (forward from −108 bp and reverse from +37 bp of NPGPx promoter, illustrated in Figure 6a). Primer sequences: forward 5′-ACATCCACC GCCTGCGGAGGG-3′ and reverse 5′-GGCTTGTTCC GGAGGTGGCGG C-3′.

Recombinant protein purification

To purify recombinant mannose-binding protein (MBP)-NCL, pNuc-1,2,3,4-RGG-C4 was transformed into BL21 codon plus bacteria, and MBP-NCL was induced by 0.5 mM IPTG at 16°C for 16 h. BL21 were pelleted and lyzed with lysis buffer (200 mM NaCl, 20 mM HEPES pH = 7.4, 1 mM EDTA, 1 mM DTT) at 4°C and lysate was clarified and incubated with amylase resin for 1 h. Resin was washed with buffer containing 1 M NaCl, 20 mM HEPES pH = 7.4, 1 mM EDTA, 1 mM DTT and MBP-NCL fusion protein was eluted with elution buffer (10 mM maltose, 1 M NaCl, 20 mM HEPES pH = 7.4, 1 mM EDTA, 1 mM DTT). MBP was purified using similar protocol. MBP-NCL and MBP were dialyzed against the buffer with 20 mM HEPES pH = 7.5 and 200 mM NaCl.

Oligonucleotides preparation

All oligonucleotides used in circular dichroism and NMR were purchased from BioBasic Inc. and used without further purification. DNA probes were resolved in solution containing 10 mM Tris–HCl (pH 7.5) and supplied with 150 mM KCl if needed. Probes were heated to 95°C for 10 min, cooled slowly to room temperature and then stored overnight at 4°C before use.

Circular dichroism

The circular dichroism (CD) spectra were averaged 10 scans on a J-815 spectropolarimeter (Jasco, Japan) with a 2-nm bandwidth at a 50-nm/min scan speed and a 0.2-nm step resolution. The CD spectra were measured under N_2 between 210 and 350 nm to ascertain the G4 structures. DNA concentration used in CD analysis was 1 μM. The DNA oligos were ordered from BioBasic Inc. (used in Figure 2) and Mission BioTech (Figure 3).

Imino proton NMR

Experiments were performed using 800 MHz Bruker spectrometers. ^{1}D NMR spectra were measured in H_2O/D_2O (90%/10%) using a jump and return sequence for solvent suppression. Strand concentration was 0.1 mM; the solution contained 10 mM Tris-HCl (pH 7.5) and 150 mM KCl, internal with reference DSS (Sodium 4,4-Dimethyl-4-silapentane-1-sulfonate).

RESULTS

Proximal NPGPx promoter contains a *cis*-element responsible for NPGPx expression enhanced by NT-siRNA

Upregulation of NPGPx transcript was found in human fibroblasts including WI38 and CAF-tert infected with lentivirus containing NT-shRNA such as shLuc (shRNA against Luciferase, Figure 1a and b), shRFP or shLacZ (26), suggesting the existence of a transcriptional regulation to modulate NPGPx expression. To investigate how NPGPx promoter responds to NT-siRNA stress, we used reporter assay to analyse NPGPx promoter activity by constructing a series of deletion mutants as illustrated in Figure 1c. In cells expressing shRFP, the NPGPx promoter reporters had higher activities compared with those in lentiviral vector transduced (shEmpty) or parental cells (Mock) (Figure 1d). The very proximal NPGPx promoter, which contains 74 nucleotides from −60 to +14, retained the robustic activity comparing with full-length or other shortened promoters (Figure 1d). These results suggest the presence of a critical *cis*-regulatory element at this region responsible for NPGPx expression under NT-siRNA stress.

NPGPx proximal promoter contains GC-rich sequences, and it is likely to form G4 structure

The NPGPx proximal promoter is highly GC-rich (85% of GC) with four potential Sp1 binding sites on the forward strand (analysed using Transfec program and TESS online). The promoter also harbors $G_{3–6}$ repeats on the backwards strand (Figure 2a), which is likely to form a G4 structure (29). Na^+/K^+ stabilizes G4 structure (1–3,30), which can be revealed by CD with a positive signal ~265 nm (31,32). To test whether NPGPx proximal promoter contains such G4 structure, we analysed the reverse strand of NPGPx proximal promoter (NPGPx-60, illustrated in Figure 2a) in the presence of K^+ by CD spectrum. As shown in Figure 2b, NPGPx-60

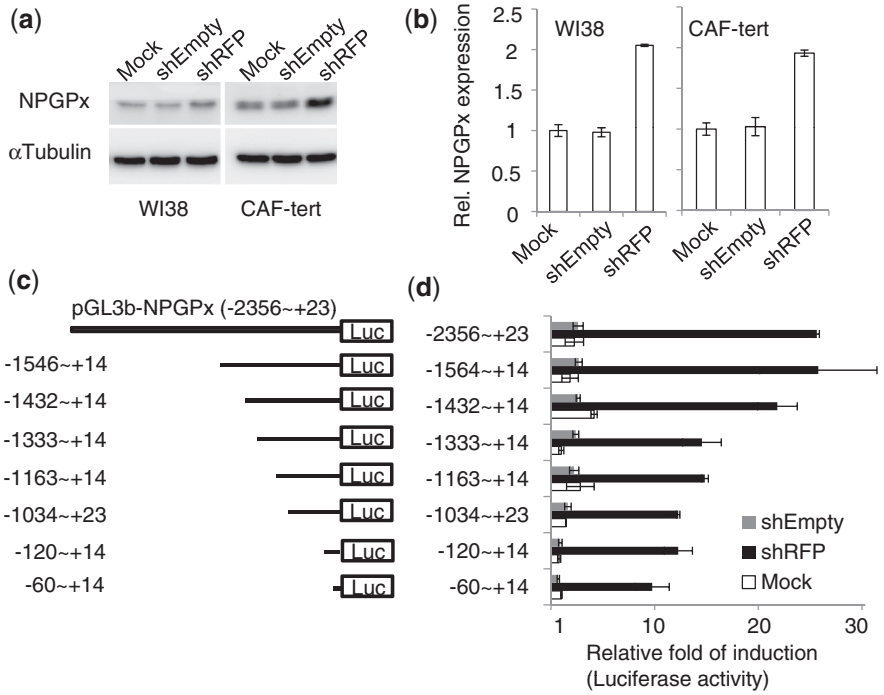

Figure 1. The proximal *cis*-element of NPGPx promoter is required for the induction of NPGPx expression in NT-siRNA-stressed cells. (**a**) Western blot analysis of NPGPx expression in WI38 or tert-immortalized human breast cancer associated fibroblast (CAF-tert) transduced with shRNA against red fluorescent protein (shRFP), or control vector (shEmpty). Antibodies against NPGPx or α-tubulin were used to probe the blot. Mock: parental cells. (**b**) Quantitative real time PCR using cells described in (a). NPGPx transcripts quantity was normalized to S26, and the relative NPGPx expression level was shown. (**c**) Schematic of NPGPx promoter constructs used in the reporter assay. (**d**) WI38 cells infected with lentiviruses carrying shRFP, shEmpty or uninfected (Mock) were transfected with NPGPx reporters described in (c) for luciferase activity assay. The luciferase activity of each reporter was compared with that of from the very proximal promoter-containing reporter (−60 to +14) in uninfected cells (mock). Each point was triplicated, and the experiments were repeated twice.

had an absorbance pick at 265 nm in the presence of K^+, indicating that the NPGPx-60 contained a potential G4 structure. Furthermore, the CD absorbance signal was mainly derived from NPGPx-32, which is composed of 32-nucleotides containing four GGG repeats from the 5′ region of NPGPx-60. In contrast, such signal was not present at the NPGPx-25, which contains 25 nucleotides with GG repeats from the 3′ region of NPGPx-60. The findings were further confirmed by NMR. When analysing the NPGPx-60 in the presence of K^+ by NMR, two individual peaks appeared (Figure 2c, bottom panel), suggesting two kinds of DNA secondary structures were found in NPGPx-60. NPGPx-25 contributed to the left-handed signal (13 ppm), whereas NPGPx-32 contributed to the right-handed signal (∼11 ppm). The NMR signal of NPGPx-32 had Hoogsteen hydrogen bonding base pairing, which may feature a specialized DNA secondary structure, G4 (13). On the other hand, the signal detected in NPGPx-25 may derive from a double-stranded pairing structure because it contains five Watson–Click base pairs and two GG pairs with hydrogen bonds (Figure 2c and e), which may form a hairpin. When the potential hairpin forming DNA sequences were mutated, the hairpin signal was diminished from NMR (Supplementary Figure S1a and b). On the other hand, NPGPx-60 in the presence of K^+ (150 mM) had higher Tm (Figure 2d), which was consistent with the presence of G4. Furthermore, the DMS footprinting analysis revealed that the G3-6 repeats of NPGPx-32 were protected in the presence of K^+ (Supplementary Figure S1c). These results together suggest that the anti-sense strand of NPGP proximal promoter contains a stable secondary structure composed of a G4 stack and a potential 3′ hairpin (Figure 2e), which may be critical for NPGPx expression in NT-siRNA-stressed cells.

The potential G4 structure is required for NPGPx upregulation on NT-siRNA stress

To elucidate the potential functional and structural relationship in NPGPx-60, we generated six individual NPGPx-60 mutants with GC to AT base substitutions (Table 1, and also illustrated in Figure 3a) at hairpin pairing site (A mutant), hairpin loop (B mutant), G4 side-chain (E mutant) and G4 column (C, D, F mutant). CD analysis of these NPGPx-60 mutants in the presence of K^+ revealed that G4 existed in mutant B and E, but not in mutant C, D and F (Figure 3b). Similar results were also obtained from NMR analysis (Figure 3c), indicating the G-rich sequences of NPGPx-60 formed G4 structure *in vitro*. Hairpin loop in mutant A was unstable, and it formed inter-molecular A–T paring (Figure 3b and c, also see Supplementary Figure S2), resulting in an unstable G4 structure.

To address the biological activities of NPGPx promoter mutants, we measure the promoter activities by using Luciferase reporters in WI38 cells expressing NT-siRNA

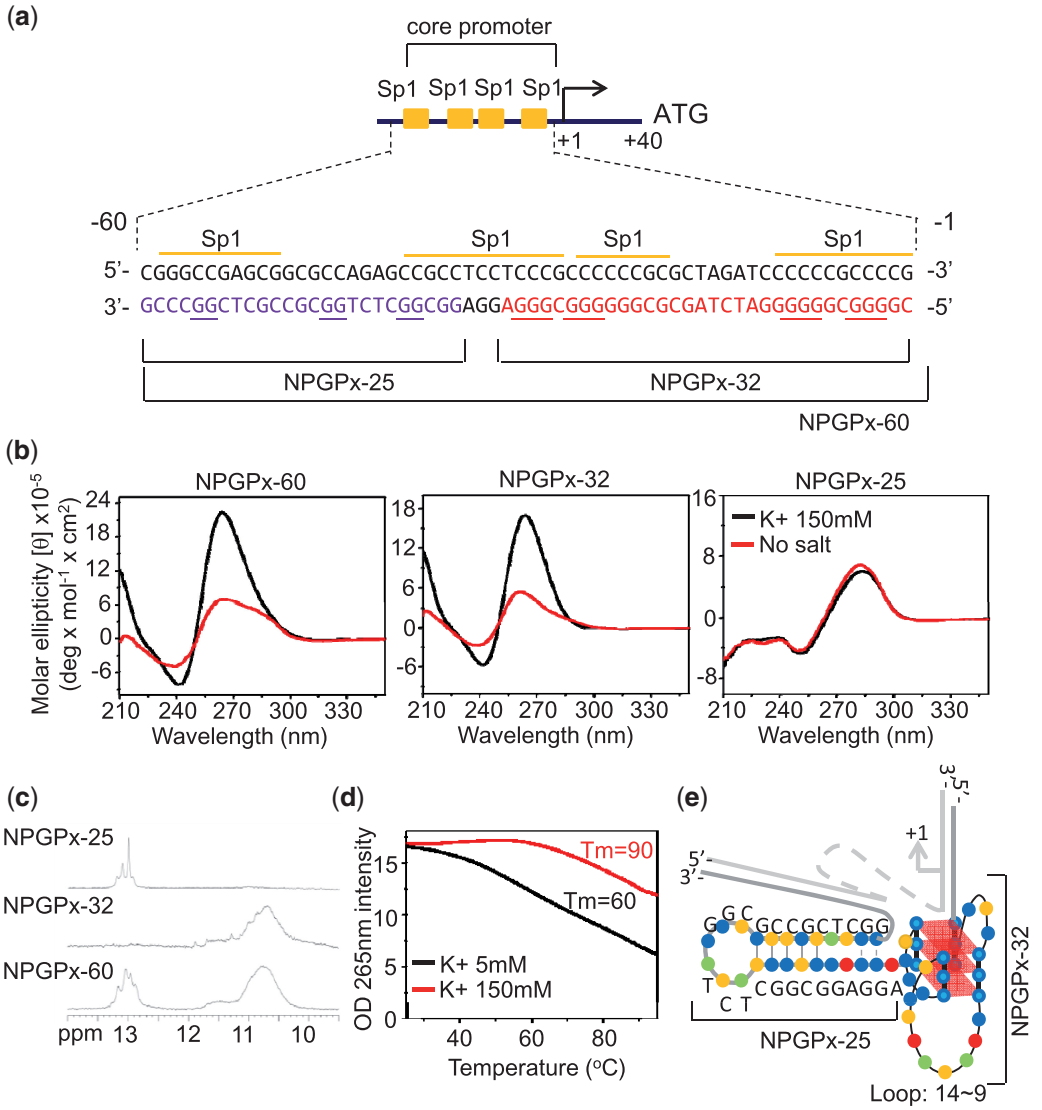

Figure 2. NPGPx proximal promoter contains a G4 DNA structure. (**a**) Schematic NPGPx proximal promoter. NPGPx proximal promoter (−60 to −1,) contains 4 putative Sp1 binding site on forward strand along with regular GG(G) repeats (G_2 repeats in NPGPx-25 and G_3 repeats in NPGPx-32) on reverse strand (named as NPGPx-60). (**b**) CD of 5 μM NPGPx-25, NPGPx-32 and NPGPx-60 with 150 mM K^+ (black line) or without K^+ (red line) at 25°C. In the presence of K^+, an absorbance at 265 nm of NPGPx-60 and NPGPx-32 was detected, and the peak was not stabilized by the presence of K^+ in NPGPx-25. (**c**) ^{1}H-NMR spectra of 0.1 mM NPGPx-25 (up), NPGPx-32 (middle) and NPGPx-60 (bottom) DNA in 150 mM K^+ solution. NPGPx-25 has the hairpin with Watson–Click hydrogen bonding base pairing, whereas NPGPx-32 has Hoogsteen hydrogen bonding base pairing. NPGPx-60 contains both structural features. (**d**) CD 265 nm melting spectra of 5 μM NPGPx-60 with 150 mM K^+ (red line) and 5 mM K^+ (black line). (**e**) Schematic the potential NPGPx-60 structure. The 3′ end of NPGPx proximal backwards promoter contains a hairpin with Watson–Click hydrogen bonding base pairing following by a G4 structure detected in NPGPx-32. A long side chain may exist between the second and the third G columns in G4 structure. These experiments have been repeated three times.

Table 1. WT and mutant NPGPx promoter sequences

Name	WT and mutant NPGPx promoter sequences (reverse, from 5′ to 3′)
WT NPGPx	cggggcgggggatctagcgcgggggcgggaggaggcggctctggcgccgctcggcccg
Mutant A	cggggcgggggatctagcgcgggggcgggaggaggcggctctggcg**ctctattattta**
Mutant B	cggggcgggggatctagcgcgggggcgggaggaggcggctc**at**gcgccgctcggcccg
Mutant C	cggggcgggggatctagcgcg**actttgttttc**gaggcggctctggcgccgctcggcccg
Mutant D	cggggcgggggatctagcgcgg**ttt**gcgggaggaggcggctctggcgccgctcggcccg
Mutant E	cggggcgggggat**aat**gcgcgggggcgggaggaggcggctctggcgccgctcggcccg
Mutant F	**gtcaagaaaa**ggatctagcgcgggggcgggaggaggcggctctggcgccgctcggcccg

The GC to AT substituted bases were underlined.

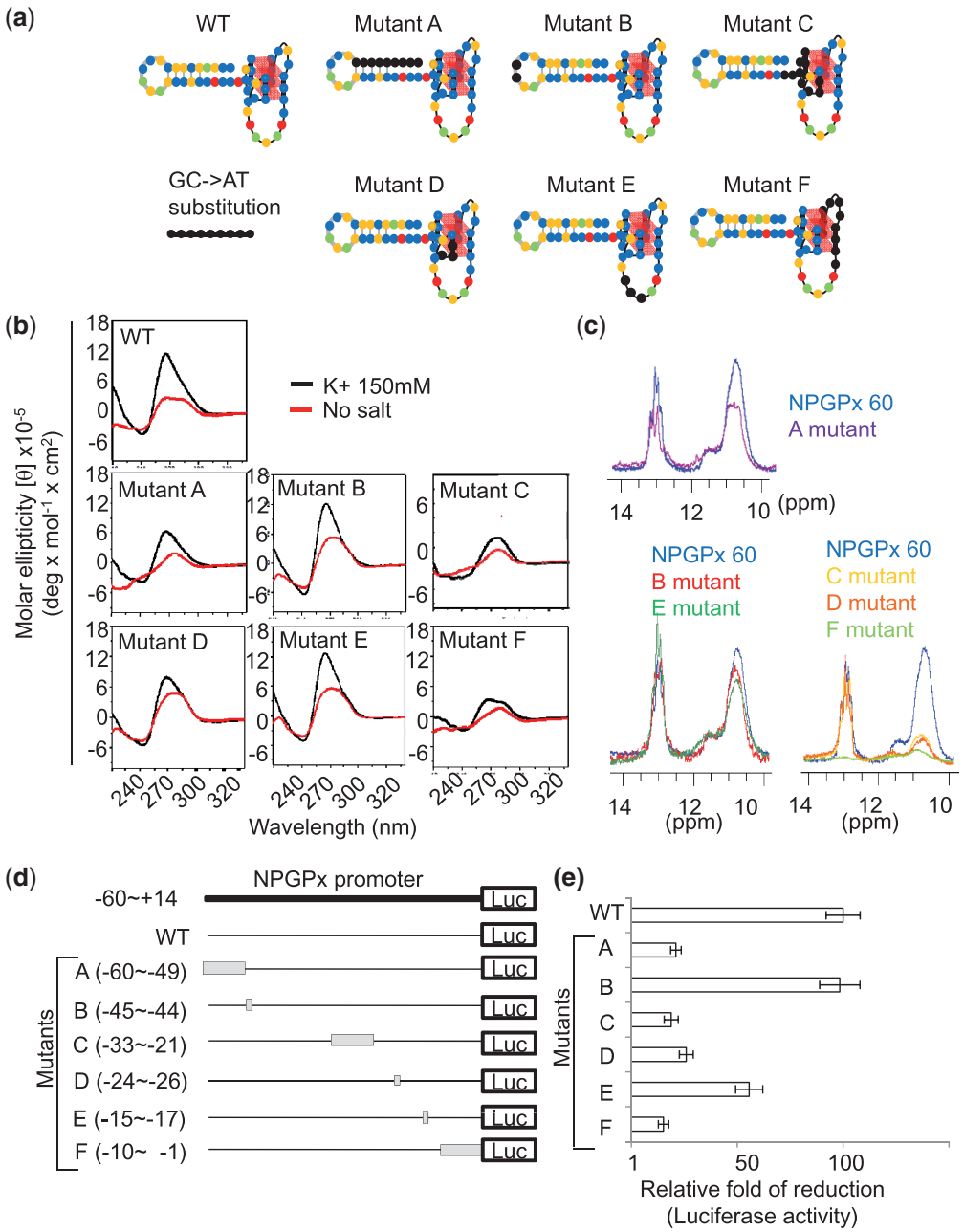

Figure 3. The G4-containing DNA structure is required for NPGPx transactivation. (**a**) Schematic NPGPx proximal backwards promoter and the designed mutants. DNA sequences of these mutants are showed in Table 1. These six mutants have bases substitution (GC to AT, labelled in black) on hairpin (Mutant A), hairpin loop (Mutant B), G4 column (Mutant C, D, F) or the long side chain between second/third G column (Mutant E). DNA sequences were shown in Table 1. (**b**) CD spectrum analysis of NPGPx proximal promoters. The G4 signal (265 nm) was diminished in mutants with base substitution on G4 column (Mutant C, D, F), whereas destroy hairpin structure destabilized G4 in Mutant A, as the 265 nm signal declines. (**c**) WT and mutant NPGPx promoters were analysed by NMR spectrum in the presence of 150 mM K^+. The spectrum of WT was either compared with Mutant A (upper), Mutant B and E (lower-left) or Mutant C, D, F (lower-right), respectively. (**d**) Schematic of WT and mutant NPGPx reporters. Grey boxed: GC to AT base substitution region. (**e**) Reporter activity assay: Each NPGPx reporter and TK-renilla reporter were co-transfected into shRFP-expression WI38 cells, and the luciferase activities were normalized to renilla activity. Reporter activities of mutants were compared with WT reporter activity. These experiments have been triplicate and repeated for three times.

(Figure 3d). B and E mutant had comparable NPGPx reporter activity to WT reporter (Figure 3e), whereas mutant A, C, D and F lost the majority of promoter activity (Figure 3e). Taken together, these data suggest that hairpin-G4 structure in NPGPx proximal promoter is essential for NPGPx upregulation responding to NT-siRNA stress.

NCL mediates NPGPx upregulation in NT-siRNA stressed cells

NCL has been shown to bind to G4 structure to activate or repress gene expression (7,22). We then tested whether NCL has a role in regulating NPGPx expression. Ectopic overexpression of NCL enhanced NPGPx reporter activity

in NT-siRNA-stressed WI38 cells (Figure 4a, shRFP compared with control vector shEmpty alone). Without NT-siRNA stress, overexpressing NCL could not enhance NPGPx reporter activity (Figure 4c, left two bars). Consistently, increasing NT-siRNA stress enhanced NPGPx reporter activity in NCL-overexpressing cells, but not in NCL-depleted cells (Figure 4c). These results suggest that NCL positively regulates NPGPx in responding to NT-siRNA stress.

Based on the above results, the *cis*-element of NPGPx-60 appears to be crucial for NPGPx transactivation (Figure 3). To test whether NCL is essential for NPGPx promoter transactivation, we measured the reporter activity of those mutants in cells expressing different amount of NCL. In NT-siRNA-stressed cells, overexpressing NCL enhanced the reporter activity of WT and mutant promoters B and E, but not mutants A, C, D and F (Figure 4e, left panel). Moreover, NPGPx promoter activities of each mutant were comparable with WT promoter in non-stressed cells (Figure 4e, right panel). Taken together, these results suggest that NCL responses to NT-siRNA stress to transactivate NPGPx promoter through its *cis*-element with G4 structure.

NCL binds to the hairpin-G4 structure of NPGPx proximal promoter

To investigate whether NCL binds to NPGPx promoter, NPGPx proximal promoter was incubated with NT-siRNA stressed nuclear extract and then subjected

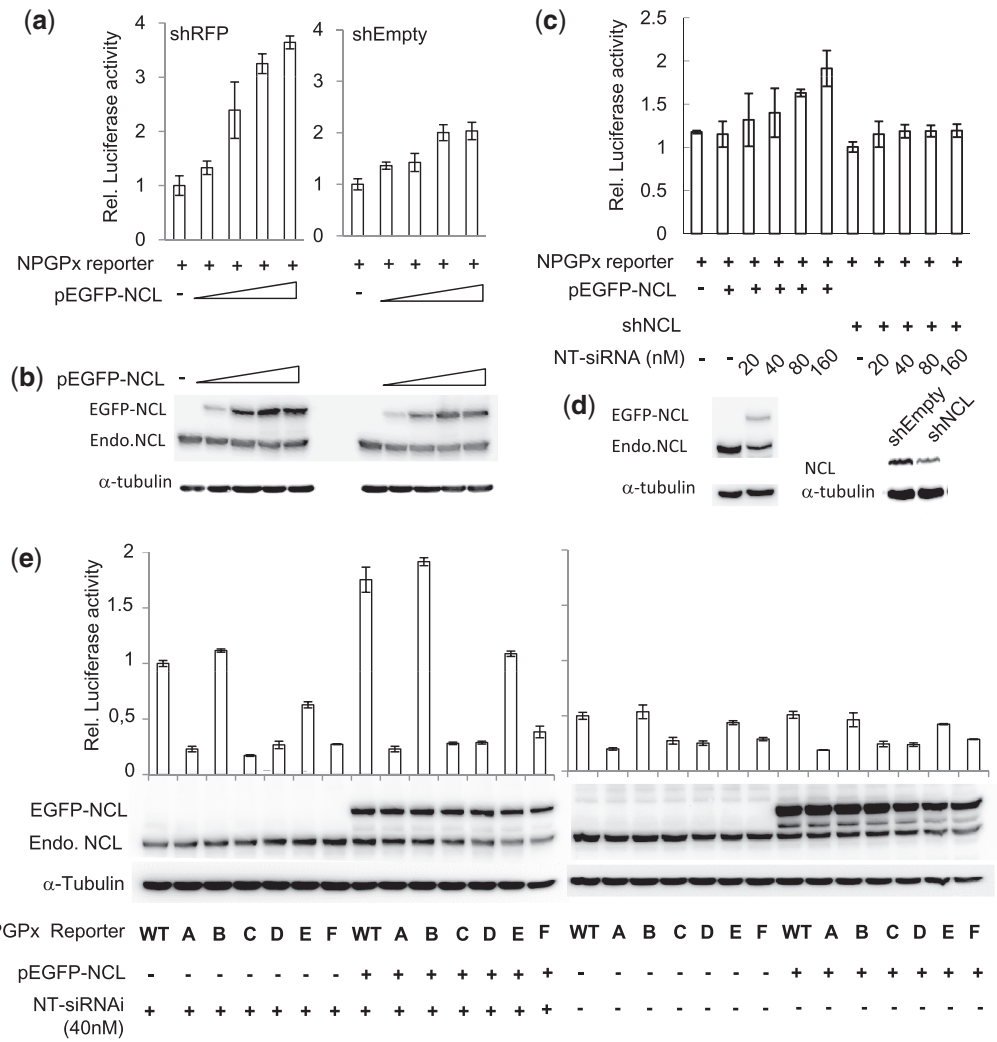

Figure 4. NCL facilitates NPGPx expression in NT-siRNA-stressed cells. (**a**) Reporter assay using WI38 cells transfected with NPGPx reporter, TK-renilla and pEGFP-NCL. Luciferase activity was normalized to renilla activity, and the relative luciferase activity was then compared with that of cells without pEGFP-NCL transfection. (**b**) Western blot analysis using cells in (a). EGFP-NCL: recombinant NCL with N-terminal EGFP tag. Endo-NCL: endogenous NCL. (**c**) Reporter assay using 293T cells transfected with NPGPx reporter, TK-renilla, NT-siRNA, pEGFP-NCL or shRNA against NCL (shNCL). Luciferase activity was normalized to renilla activity, and the relative luciferase activity was then compared with that of cells without pEGFP-NCL transfection. (**d**) Western blot analysis using cells from (c). (**e**) Reporter assay using 293T cells transfected with TK-renilla, NT-siRNA, pEGFP-NCL accompany with WT or mutant NPGPx reporters. Luciferase activity was normalized to renilla activity, and the relative luciferase activity was then compared to that of cells with NT-siRNA transfection. NCL protein was bloted, and the quantities were showed in below. α-tubulin: internal control. These experiments have been triplicate and repeated three times.

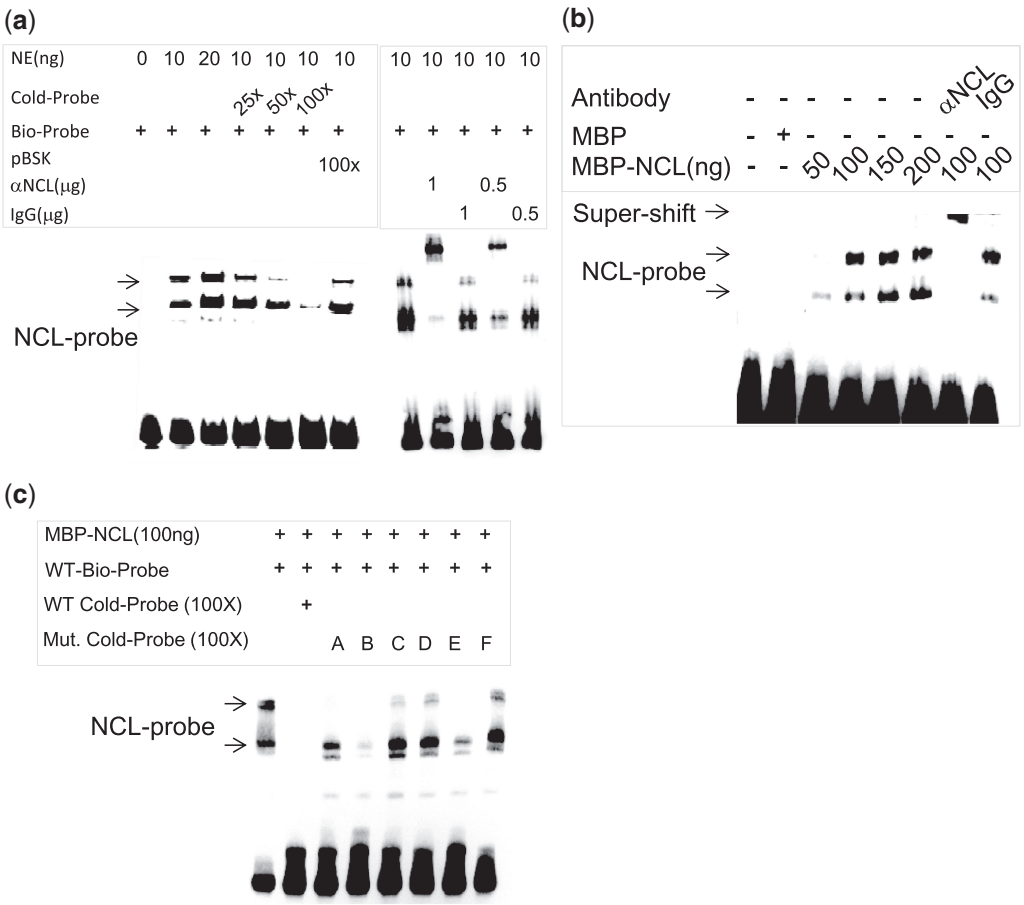

Figure 5. NCL binds to NPGPx proximal promoter *in vitro*. (**a**) EMSA experiment. Biotinylated NPGPx proximal promoter (Bio-probe) was incubated with nucleus extract from NT-siRNA-stressed cells. NPGPx probe-protein complex were separated in non-denature TBE-PAGE and visualized by anti-biotin Ab in EMSA. Cold-probe: non-biotinylated NPGPx promoter; pBSK: scramble unlabeled DNA fragment; αNCL: antibody against NCL; IgG: control mouse IgG. (**b**) EMSA experiment. Biotinylated NPGPx proximal promoter (Bio-probe) was incubated with purified recombinant MBP-tagged NCL (MBP-NCL), and DNA-NCL complex were probed after EMSA procedure. MBP: mannose-binding protein. (**c**) Competition EMSA experiment. Unlabelled NPGPx promoters, WT or mutants were compete with biotinylated NPGPx promoter for NCL binding in EMSA experiment. The upper shift was competed by WT, mutant A, B, E probe, whereas the lower complex could only removed by WT and mutant B probe competition. These experiments have been repeated for three times.

to EMSA. Two major band-shifts containing NPGPx promoter were detected (Figure 5a). To test whether the DNA–protein complex contains NCL, we treated the mixture with anti-NCL antibody and detected these two bands were super-shifted (Figure 5a, right). Next, we tested whether NCL directly binds to NPGPx promoter *in vitro* by using purified recombinant NCL and biotinlylated NPGPx promoter DNA in EMSA experiment (Figure 5b). Similar band shifting patterns were observed, suggesting that NCL specifically binds to NPGPx proximal promoter.

To further dissect the importance of each DNA secondary structure (hairpin or G4) in terms of DNA–NCL interaction, we used unlabeled NPGPx mutant promoters (A–F) as competition probe in EMSA experiments. As shown in Figure 5c, the upper band was effectively competed out by WT, mutant A, B and E probes, whereas only unlabelled WT, B and E mutant probes could efficiently competed out the lower band. The mutant C, D and F probes failed to compete out with these two bands. These results suggest that NCL has dynamic preferences to bind to the mixed (stem loop-containing) G4 structure of NPGPx promoter.

NCL replaces Sp1 to bind NPGPx proximal promoter on NT-siRNA stress

To explore how NCL binds to NPGPx promoter *in vivo*, we performed ChIP assay with antibodies against NCL using NT-shRNA-stressed WI38 cells (illustrated in Figure 6a). As shown in Figure 6b, NCL is bound to NPGPx proximal promoter in NT-siRNA-stressed cells, but not in control cells. On the contrary, NPGPx promoter contains putative Sp1-binding sites (illustrated in Figure 2a), and the ChIP assay revealed that Sp1 was released from NPGPx proximal promoter on NT-siRNA stress (Figure 6c). These results implicate that NCL was recruited to NPGPx promoter to replace Sp1 by binding to stem loop/G4 structure when cells were under NT-siRNA stress.

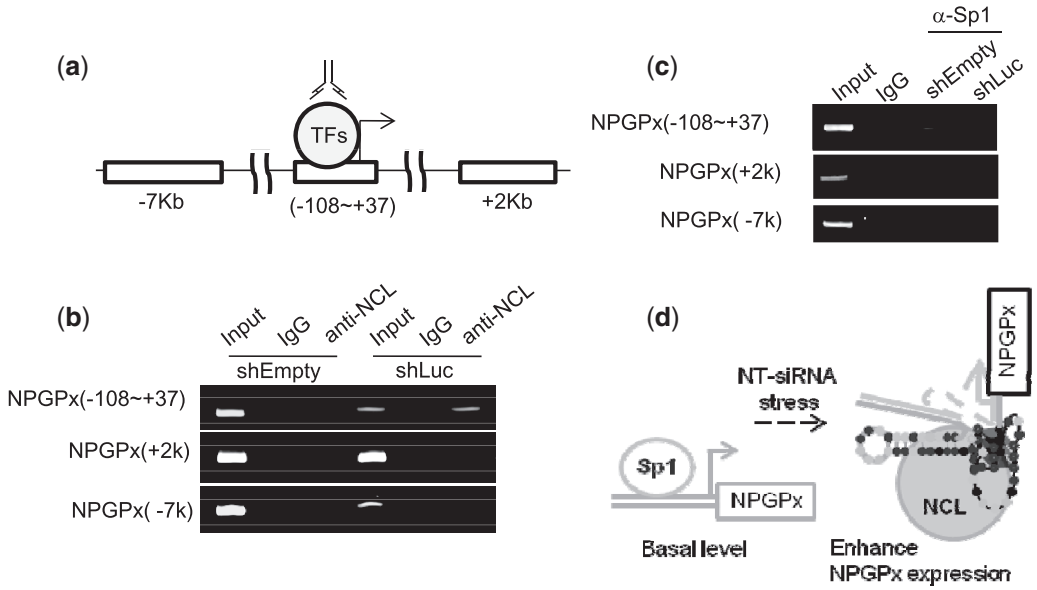

Figure 6. NCL binds to NPGPx proximal promoter in NT-siRNA-stressed cells. (**a**) Schematic of NPGPx genomic DNA region. Square boxes indicated the DNA region amplified by PCR in ChIP assay. (**b**) ChIP assay. WI38 cells transduced with shLuc or control vector (shEmpty) were used for ChIP assay with antibody against NCL. The proximal NPGPx promoter region (−108 to +14) was amplified by PCR following ChIP assay. PCR products amplified from far 7-kb upstream or 2-kb downstream of NPGPx were used as negative controls. Mouse IgG: negative control. (**c**) ChIP assay. Sp1 and its interacting DNA were pull downed from WI38 cells described in (b), and the NPGPx promoter DNA was quantitated by PCR. ChIP experiments are repeated for three times individually. (**d**) Proposed model of NPGPx transactivation in NT-siRNA-stressed cells. In normal condition, Sp1 maintains NPGPx expression in a basal level. When cells were suffered from NT-siRNA stress, NCL replaced the Sp1 binding on the positive strand of the hairpin-G4 sequences and transactivated NPGPx to release the accumulated NT-siRNAs.

DISCUSSION

A mixed type G4 structure may be present in NPGPx promoter

In this communication, we provided evidence to support the possibility that NPGPx proximal promoter contains a mixed type of G4, which is required for NPGPx transactivation on NT-siRNA stress. When G was substituted into A/T in the predicted G columns (Mutant C, D, F in Figure 3b and c), the G4 structure was diminished from CD and NMR readout. The NMR spectrum result revealing a broad, instead of sharp, G4 signal at ppm11 of NPGPx-32 (Figure 2c), which suggests NPGPx promoter may simultaneously contains dynamic G4 structures. As the G4 stack only requires four repeats of GGG, the dynamic forms of G4 may derive from different preference of G usage of the second and third G columns in which are 5–6 series of G in a row. On the other hand, NMR spectra of NPGPx-25 showed a signal between 12 and 14 ppm, but not in NPGPx-32, and it may represent an intra-molecular base pairing. The 12–14 ppm signal revealed by NMR spectrum represents Watson–Click pairing, which is not interfered by K^+ concentration, and one of the most possible structures made by single strand DNA is a hairpin. It was noticed that the G4 was destabilized when the hairpin structure was perturbed as seen in mutant A (Figure 3b and c). One possible explanation is that mutant A formed inter-molecular base paring *in vitro* (Supplementary Figure S1), which may interfere G4 formation and reduce either NMR or CD intensity of G4 readout. These data strongly suggest that a non-canonical G4 with hairpin in 3′ end may be present at the NPGPx proximal promoter.

NCL binds to the G4 structure of NPGPx proximal promoter to regulate its transcription

Based on the analysis of the functional and structural relationship, NPGPx promoter mutants with compromised hairpin-G4 stability had diminished transactivation activity of NPGPx promoter on NT-siRNA stress (Figure 3). However, mutations occurred on the side chain or hairpin loop (mutant B and E, illustrated in Figure 2a) had little effect on the promoter activity. These results indicate the importance of the G4-hairpin structure for transcriptional regulation of the NPGPx promoter. Similar G4 with hairpin structure has been found in the promoter of VEGF (22). On the other hand, c-Myc contains several hairpin-free canonical G4 structure with short side chain in its promoter, and those G4s are important for c-Myc repression (7). Although the precise mechanism is not available for explaining the diverse activity of these two G4 structures, several intrinsic differences may contribute to these differences; one is the relative location of the G4 to the transcriptional starting site. The mixed G4 located in the negative strand just following NPGPx transcription starting site, whereas the G4 in c-Myc promoter is relatively far away from the transcriptional starting site. It is likely that the binding of NCL to the mixed G4 may stabilize the reverse strand to maintain dsDNA opening puff and facilitate transcription from the positive strand of NPGPx coding sequences as described in the model

(Figure 6d), whereas the binding of NCL to the G4 in Myc promoter blocks transcription. The other possibility lies on the structural difference, which may provide distinct docking site for different set of NCL/transcriptional factors. As shown in Figure 5c, two different DNA-NCL complexes exist in EMSA. The upper band possibly contains G4-NCL complex, as this band can be compete by probe without hairpin structure (mutant A). The lower band may contain hairpin-G4-NCL complex, which cannot be competed out by mutants without either hairpin or G4 (Mutant A, C, D, F). The hairpin-G4-NCL complex appears to be more compact than the G4-NCL one, as it has a higher mobility in native gel, reflecting a different tertiary structure. These distinct bands may be reflected by diverse G4-structures for different transcriptional complex to bind. Alternatively, these two different bands seen in EMSA may contain different stoichiometry of DNA-NCL complexes. Although the latter possibility is not fully compatible with the results of Figure 5, the precise binding mechanism remains to be explored. On the other hand, NCL could also cooperate with other transcriptional factor(s) for binding to the G4 structure of NPGPx promoter. It was noted that NCL binds to c-Jun to transactivate downstream genes (23). However, our preliminary data showed that c-Jun was not recruited to NPGPx proximal promoter in NT-siRNA-stressed cells (Supplementary Figure S2), suggesting that NCL may have other co-transactivators. Thus, it will be of interest to pursue whether any other co-factor associated with NCL for binding to the mixed G4 structure of NPGPx promoter accounts for their distinct transcriptional regulations.

How NCL responds to NT-siRNA stress to facilitate NPGPx transactivation?

It has been reported that NCL was translocated from nucleolus to nucleoplasm in IR or UV-irradiated cells (24). Intriguingly, the translocation of NCL on IR stress coincided with its post-translational modifications, such as phosphorylation (25). Our preliminary data showed that the amount of phosphorylated NCL (p-NCL) was increased in NT-siRNA-stressed cells (Supplementary Figure S3a) and the p-NCL bound to the wild-type NPGPx proximal promoter (Supplementary Figure S3b and d), but not the G4 mutant (mutant D) (Supplementary Figure S3c), suggesting a correlation between NT-siRNA stress and NCL phosphorylation. Although the precise role of p-NCL in gene transcription remains obscure; one possibility is that the phosphorylated NCL can be shuttled from nucleolus to nucleoplasm and bind to its targeted structure such as mixed hairpin/G4 structure. The other is the p-NCL may recruit other transcription co-factors to bind to mixed hairpin/G4 structure, and these two possibilities are not mutual exclusive.

We also observed that NCL may compete with Sp1 to bind to NPGPx proximal promoter (Figure 6) and transactivated NPGPx in NT-siRNA-stressed cells. This is consistent with the previous observation that the p-NCL competes with chromatin silencing complex REST to activate gene expression (21). Notably, the N-terminus of NCL enriches with Ser/Thr and can be phosphorylated by CKII (21) or PKC (33). Though the upstream kinases responsible for NCL phosphorylation remain to be explored, our evidences suggested that NCL is important for upregulation of NPGPx expression on NT-siRNA stress.

SUPPLEMENTARY DATA

Supplementary Data are available at NAR Online: Supplementary Figures 1–4 and Supplementary Methods.

ACKNOWLEDGEMENTS

The authors thank Professor Nancy Maizel and Professor Joseph T. Tseng for their generosity to share the NCL expression vectors. According to UCI policy, W.H.L. declares that he serves as a board member of GeneTex, a biotech company. This arrangement has been reviewed and approved by UCI COI committee.

FUNDING

This work was mainly supported by the funds from the Academia Sinica, Taiwan. Funding for open access charge: The Academia Sinica, Taiwan.

Conflict of interest statement. None declared.

REFERENCES

1. Lipps,H.J. and Rhodes,D. (2009) G-quadruplex structures: in vivo evidence and function. *Trends Cell Biol.*, **19**, 414–422.
2. Sen,D. and Gilbert,W. (1988) Formation of parallel four-stranded complexes by guanine-rich motifs in DNA and its implications for meiosis. *Nature*, **334**, 364–366.
3. Williamson,J.R., Raghuraman,M.K. and Cech,T.R. (1989) Monovalent cation-induced structure of telomeric DNA: the G-quartet model. *Cell*, **59**, 871–880.
4. Yang,D. and Okamoto,K. Structural insights into G-quadruplexes: towards new anticancer drugs. *Future Med. Chem.*, **2**, 619–646.
5. Shimizu,A. and Honjo,T. (1984) Immunoglobulin class switching. *Cell*, **36**, 801–803.
6. Kilpatrick,M.W., Torri,A., Kang,D.S., Engler,J.A. and Wells,R.D. (1986) Unusual DNA structures in the adenovirus genome. *J. Biol. Chem.*, **261**, 11350–11354.
7. Gonzalez,V. and Hurley,L.H. (2010) The C-terminus of nucleolin promotes the formation of the c-MYC G-quadruplex and inhibits c-MYC promoter activity. *Biochemistry*, **49**, 9706–9714.
8. De Armond,R., Wood,S., Sun,D., Hurley,L.H. and Ebbinghaus,S.W. (2005) Evidence for the presence of a guanine quadruplex forming region within a polypurine tract of the hypoxia inducible factor 1alpha promoter. *Biochemistry*, **44**, 16341–16350.
9. Sun,D., Guo,K., Rusche,J.J. and Hurley,L.H. (2005) Facilitation of a structural transition in the polypurine/polypyrimidine tract within the proximal promoter region of the human VEGF gene by the presence of potassium and G-quadruplex-interactive agents. *Nucleic Acids Res.*, **33**, 6070–6080.
10. Cogoi,S. and Xodo,L.E. (2006) G-quadruplex formation within the promoter of the KRAS proto-oncogene and its effect on transcription. *Nucleic Acids Res.*, **34**, 2536–2549.
11. Dai,J., Dexheimer,T.S., Chen,D., Carver,M., Ambrus,A., Jones,R.A. and Yang,D. (2006) An intramolecular G-quadruplex structure with mixed parallel/antiparallel G-strands formed in the

human BCL-2 promoter region in solution. *J. Am. Chem. Soc.*, **128**, 1096–1098.
12. Blackburn,E.H. (1984) The molecular structure of centromeres and telomeres. *Annu. Rev. Biochem.*, **53**, 163–194.
13. Burge,S., Parkinson,G.N., Hazel,P., Todd,A.K. and Neidle,S. (2006) Quadruplex DNA: sequence, topology and structure. *Nucleic Acids Res.*, **34**, 5402–5415.
14. Palumbo,S.L., Ebbinghaus,S.W. and Hurley,L.H. (2009) Formation of a unique end-to-end stacked pair of G-quadruplexes in the hTERT core promoter with implications for inhibition of telomerase by G-quadruplex-interactive ligands. *J. Am. Chem. Soc.*, **131**, 10878–10891.
15. Siebenlist,U., Hennighausen,L., Battey,J. and Leder,P. (1984) Chromatin structure and protein binding in the putative regulatory region of the c-myc gene in Burkitt lymphoma. *Cell*, **37**, 381–391.
16. Simonsson,T., Pecinka,P. and Kubista,M. (1998) DNA tetraplex formation in the control region of c-myc. *Nucleic Acids Res.*, **26**, 1167–1172.
17. Tomonaga,T. and Levens,D. (1996) Activating transcription from single stranded DNA. *Proc. Natl Acad. Sci. USA*, **93**, 5830–5835.
18. Bossone,S.A., Asselin,C., Patel,A.J. and Marcu,K.B. (1992) MAZ, a zinc finger protein, binds to c-MYC and C2 gene sequences regulating transcriptional initiation and termination. *Proc. Natl Acad. Sci. USA*, **89**, 7452–7456.
19. Siddiqui-Jain,A., Grand,C.L., Bearss,D.J. and Hurley,L.H. (2002) Direct evidence for a G-quadruplex in a promoter region and its targeting with a small molecule to repress c-MYC transcription. *Proc. Natl Acad. Sci. USA*, **99**, 11593–11598.
20. Seenisamy,J., Rezler,E.M., Powell,T.J., Tye,D., Gokhale,V., Joshi,C.S., Siddiqui-Jain,A. and Hurley,L.H. (2004) The dynamic character of the G-quadruplex element in the c-MYC promoter and modification by TMPyP4. *J. Am. Chem. Soc.*, **126**, 8702–8709.
21. Gonzalez,V., Guo,K., Hurley,L. and Sun,D. (2009) Identification and characterization of nucleolin as a c-myc G-quadruplex-binding protein. *J. Biol. Chem.*, **284**, 23622–23635.
22. Uribe,D.J., Guo,K., Shin,Y.J. and Sun,D. (2011) Heterogeneous nuclear ribonucleoprotein K and nucleolin as transcriptional activators of the vascular endothelial growth factor promoter through interaction with secondary DNA structures. *Biochemistry*, **50**, 3796–3806.
23. Tsou,J.H., Chang,K.Y., Wang,W.C., Tseng,J.T., Su,W.C., Hung,L.Y., Chang,W.C. and Chen,B.K. (2008) Nucleolin regulates c-Jun/Sp1-dependent transcriptional activation of cPLA2alpha in phorbol ester-treated non-small cell lung cancer A549 cells. *Nucleic Acids Res.*, **36**, 217–227.
24. Daniely,Y., Dimitrova,D.D. and Borowiec,J.A. (2002) Stress-dependent nucleolin mobilization mediated by p53-nucleolin complex formation. *Mol. Cell Biol.*, **22**, 6014–6022.
25. Kim,K., Dimitrova,D.D., Carta,K.M., Saxena,A., Daras,M. and Borowiec,J.A. (2005) Novel checkpoint response to genotoxic stress mediated by nucleolin-replication protein a complex formation. *Mol. Cell Biol.*, **25**, 2463–2474.
26. Wei,P.C., Lo,W.T., Su,M.I., Shew,J.Y. and Lee,W.H. (2011) Non-targeting siRNA induces NPGPx expression to cooperate with exoribonuclease XRN2 for releasing the stress. *Nucleic Acids Res.*, **40**, 323–332.
27. Dignam,J.D., Lebovitz,R.M. and Roeder,R.G. (1983) Accurate transcription initiation by RNA polymerase II in a soluble extract from isolated mammalian nuclei. *Nucleic Acids Res.*, **11**, 1475–1489.
28. Hwang-Verslues,W.W. and Sladek,F.M. (2008) Nuclear receptor hepatocyte nuclear factor 4alpha1 competes with oncoprotein c-Myc for control of the p21/WAF1 promoter. *Mol. Endocrinol.*, **22**, 78–90.
29. Huppert,J.L. and Balasubramanian,S. (2007) G-quadruplexes in promoters throughout the human genome. *Nucleic Acids Res.*, **35**, 406–413.
30. Sundquist,W.I. and Klug,A. (1989) Telomeric DNA dimerizes by formation of guanine tetrads between hairpin loops. *Nature*, **342**, 825–829.
31. Kypr,J., Kejnovska,I., Renciuk,D. and Vorlickova,M. (2009) Circular dichroism and conformational polymorphism of DNA. *Nucleic Acids Res.*, **37**, 1713–1725.
32. Gray,D.M., Wen,J.D., Gray,C.W., Repges,R., Repges,C., Raabe,G. and Fleischhauer,J. (2008) Measured and calculated CD spectra of G-quartets stacked with the same or opposite polarities. *Chirality*, **20**, 431–440.
33. Zhou,G., Seibenhener,M.L. and Wooten,M.W. (1997) Nucleolin is a protein kinase C-zeta substrate. Connection between cell surface signaling and nucleus in PC12 cells. *J. Biol. Chem.*, **272**, 31130–31137.